Self-powered Gate Drive Circuits with Optical Signal Isolation for In-vehicle Marx Circuit of Ozonizer

Keisuke Kusaka, *Member, IEEE*, Yosuke Ouchi, *Non-member,* and Jun-ichi Itoh, *Senior-Member, IEEE*

***Abstract*—Reducing the cost of a Marx circuit as a high-voltage power supply for NOx decomposition for diesel vehicles is required. The Marx circuit with MOSFETs has an advantage in size compared to the Marx circuit with gap switches. However, the Marx circuit with MOSFETs needs gate drive circuits on the gate of each MOSFET. The gate signal and drive power must be supplied to each gate with isolation in a low-cost way. However, the transformer for the isolation with high-withstand voltage, such as 10 kV or more, is typically high cost because of the low demand.**

This paper proposes the self-powered gate drive circuit using the charging path of the Marx circuit. The proposed gate drive circuit only requires a low withstand voltage because the power for the MOSFET on the *n*-th stage is supplied from the (*n* - 1)-th stage via a low-voltage transformer. Besides, the gate signal is transmitted through pairs of LEDs and photodiodes instead of high-cost optical fibers. The proposed gate drive circuits are developed and implemented into a prototype of the Marx circuit with an output voltage of 4 kV. From the experiments, it is demonstrated that the proposed drive circuits provide both drive power and gate signal.

***Index Terms*—Driver circuits, pulse power systems, isolation technology**

I. Introduction

In recent years, nitrogen oxide (NOx) gas emitted by diesel vehicles has been a critical issue because it accelerates global warming. In response to this, the regulations on NOx gas emission have been tightening in each country or region. Thus, reducing NOx gas emissions is a crucial problem for automotive companies. A lean NOx trap catalyst (LNT catalyst) has been used to reduce the emission of NOx gas [1]. However, the performance of the catalyst deteriorates when the exhaust gas temperature is low. The performance degradation leads to the risk of not satisfying emission regulations. In order to improve the performance of the catalyst even in low exhaust gas temperature, mounting ozonizers onto the diesel vehicle is one of the solutions to help NOx decomposition [2–3]. The generated ozone reforms NO into NO_2, which is highly reactive by the LNT catalyst.

The Marx circuit is used as a power supply for the ozonizer [4–7]. The Marx circuit outputs high voltage by switching the connection of Marx capacitors on each cell from the parallel to the series connection. Especially, silicon carbide (SiC) MOSFETs have been used in the Marx circuit with the progress of SiC semiconductor technology in recent years instead of mechanical switches or conventional silicon (Si) MOSFETs. A SiC-MOSFET provides a good feature to the Marx circuit that a SiC-MOSFET achieves a fast switching of high-voltage devices, such as 1.2 or 1.7 kV, due to their high electron mobility and high bandgap voltage [8–9]. The fast switching improves ozone production performance.

The Marx circuit with semiconductor switches has the gate drive circuits for each MOSFET. Each gate drive circuit requires an isolated power supply for the gate drive and isolated signal transmission function, which communicates with the central controller to adjust the switching timings of the MOSFETs. In the Marx circuit, high voltage isolation is required because the source terminal voltage of each MOSFET becomes high when the Marx capacitors are connected in series.

For signal isolation, optocouplers are used in the field of low-voltage power electronics. However, the typical value of common-mode reduction (CMR) is less than 50 kV/μs. The CMR of the optocouplers is not enough to employ the SiC-MOSFET, which turns on and off with less than ten nanoseconds, for a 10-kV output voltage of the Marx circuit. For high-voltage applications in power electronics, optical fibers are also used. However, an *n*-stage Marx circuit requires $2n$ optical fibers[1]. In automotive applications, many optical fibers are not a realistic option from a cost and reliability perspective.

In terms of drive power of MOSFETs, the isolated DC-DC converters with high withstand voltage between the primary and secondary sides must be employed because the drain voltage of the high-side MOSFETs rapidly varies due to the operation of the Marx circuit. The typical withstand voltage between the DC-DC converter is less than 5 kV. Thus, the reinforced insulated DC-DC converters with high-withstand

This paragraph of the first footnote will contain the date on which you submitted your paper for review.

K. Kusaka is with Nagaoka University of Technology, Nagaoka, Niigata, Japan (e-mail: kusaka@vos.nagaokaut.ac.jp).

Y. Ouchi is with Nagaoka University of Technology, Nagaoka, Niigata Japan (e-mail: s195026@stn.nagaokaut.ac.jp).

J. Itoh is with Nagaoka University of Technology, Nagaoka, Niigata, Japan (e-mail: itoh@vos.nagaokaut.ac.jp).

[1]The classical Marx circuit, which has a switch, Marx capacitor, and resistances on each stage, needs only n optical fibers. However, the Marx circuit with two switches on each stage is discussed from the standpoint of efficiency.

voltage must be used for the Marx circuit with 10 kV or more output voltage. It is also not a realistic option from a cost perspective. In [10–11], the self-powered gate drive system has been proposed. The gate drive power is supplied with the gate signal through a pulse transformer. However, the transformers used in the *j*-th stage must have a withstand voltage *j* times greater than the input voltage.

This paper proposes a self-powered gate drive circuit with a low-voltage transformer, which supplies gate drive power from (*n*-1)-th stage to *n*-th stage, to reduce the required isolation voltage and cost of the gate driver circuits. The low-voltage transformer can be employed for the gate drive power supply in the proposed circuit. Besides, the gate signal is communicated by pairs of LEDs and photodiodes with an air gap of 50 mm. Due to these gate drive circuit configurations, the cost of the gate drive power supply for the in-vehicle Marx circuit is reduced. The rest of this paper is as follows. First, the circuit configuration of the Marx circuit and its gate drive circuits are explained. Next, the design of the transformer for the power supply is discussed. Finally, a 4-kV prototype with the proposed gate drive circuits is demonstrated.

II. Gate Drive Circuit for Marx Circuit

A. Circuit Configuration

Fig. 1 shows the *n*-stage Marx circuit with the proposed gate drive circuits. The Marx circuit has multiple stages with two MOSFETs, the diode and the Marx capacitors. When the switches for a charge S_{Cn} turns-on, the Marx capacitors are connected in parallel. The Marx capacitors are charged by the input voltage V_{in} through the diodes D_n. When the switches for a discharge S_{Dn} are on, the Marx capacitors are connected in series. The high voltage is applied to the load. The MOSFETs are turned on or off by the gate drive circuits connected between the gate and source terminal. The gate drive circuits need auxiliary power with the isolation for the gate drive because the source terminals of the MOSFETs are dynamically changed by the switching.

In the proposed circuit, the drive power is supplied from the transformers, which are connected to the low-level stage. The rush current for charging operation is suppressed by the transformers because the transformers are on only the charging path of the Marx circuit. In other words, the discharging operation of the Marx circuit is not affected by the transformer. Besides, the gate signal must be transmitted from the central controller on a low-voltage side to the gate drive circuits with signal isolation. The isolation distance between the controller on the low-voltage side and the high-voltage side must be ensured to satisfy the safety standard, such as IEC60664-1.

B. Gate Drive Circuits with Isolation

Fig. 1(b) shows the details of the gate drive circuits of the Marx circuit, as shown in Fig. 1 (a). Fig. 1(b) is illustrated by focusing on one set of switches S_{Cn}, S_{Dn}, and its gate drive circuits. In Fig. 1(b), the thick wires are part of the main path of the Marx circuit. Other lines are for gate drive. Fig. 1(c) shows the prototype. On the main circuit side, each PCB has a three-

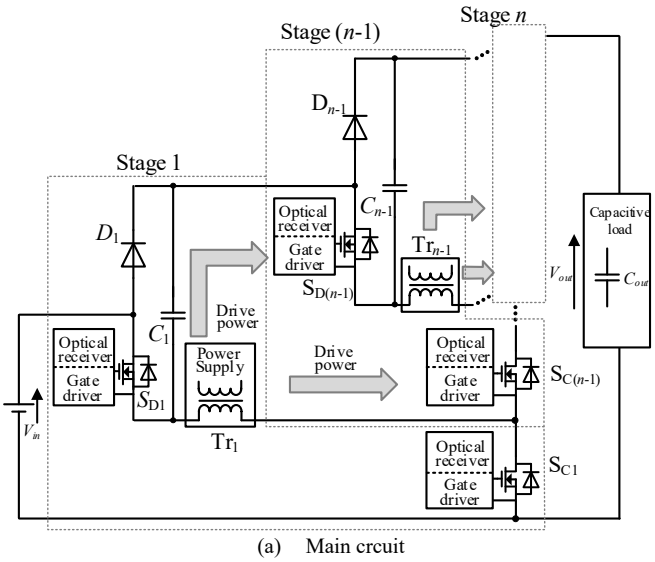

(a) Main crcuit

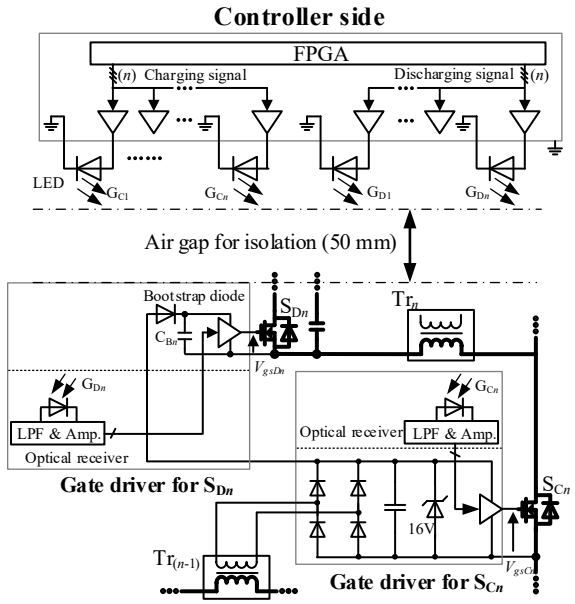

(b) Self-powered gate drive circuits and signal transmission with optical isolation

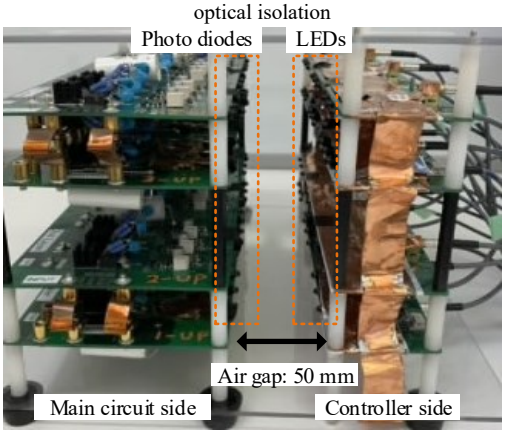

(c) Prototype for signal transmission with isolation

Fig. 1. Marx circuit with proposed gate drive circuits.

stage Marx circuit and six gate drive circuits with the optical receivers. On the controller side, six amplifiers and LEDs are mounted on each PCB. On the low-voltage side, the controller outputs two kinds of signals. One is the charging signal for the MOSFETs S_{Cn}. The other is the discharging signal for the MOSFETs S_{Dn}. The signals are amplified to drive the LEDs, which emit invisible light. The optical signal is transmitted from the controller to each gate drive circuit via an air gap of 50 mm. The air gap plays a role in electric isolation. The optical receiver on each gate drive circuit detects the optical signal with the photodiode, which has the same wavelength band as the wavelength of LED. The detected gate signal is amplified and used to drive the MOSFETs in the gate drive circuit. The pairs of LED and photodiode are cost-effective in comparison with optical fiber, mainly for automotive applications. The required footprints of the diodes and LEDs do not significantly change from the transmitter and receiver of the optical fibers. However, it should be noted that the degree of freedom of installation of LEDs and photodiodes is inferior to that of the optical fiber because the LEDs and photodiodes must be placed on the same plane.

The drive power for S_{Cn} and S_{Dn} is supplied through the transformers $Tr_{(n-1)}$, as shown in Fig. 1 (b). At the start of the charging operation of the Marx circuit, the rush current flows through D_{n-1}, C_{n-1}, $Tr_{(n-1)}$, and $S_{C(n-1)}$. The current charges the Marx capacitor during the charging operation. The induced voltage on the secondary side of $Tr_{(n-1)}$ is rectified in the gate drive circuit. The DC voltage is clamped and maintained at 16 V by the Zener diode.

Besides, the DC line of the gate drive circuit for $S_{C(n-1)}$ is connected to the drive circuit for $S_{D(n-1)}$ through the bootstrap diode. During the charging operation, the current for the drive flows through the bootstrap diode and bootstrap capacitor $C_{B(n-1)}$, $Tr_{(n-1)}$, and $S_{C(n-1)}$.

The gate drive circuit for S_{Dn} is driven using the charge of the bootstrap capacitor $C_{B(n-1)}$ as a power supply. It is the same operation as the bootstrap gate-drive circuit for inverters [12–13]. Note that the bootstrap diode plays a role in preventing the reverse voltage to the gate drive circuit from the main circuit. Thus, the reverse blocking voltage of the bootstrap diode must be higher than the DC voltage of each Marx capacitor.

Note that the isolated power supply is required in the gate drive circuit for only S_{C1} and S_{D1} for a start-up of the Marx circuit. The required isolation voltage for these switches is relatively small because the maximum voltage potential of the source terminals of the S_{D1} and S_{C1} is equal to the input voltage and zero, respectively.

At the start-up of the Marx circuit, only the two switches S_{C1} and S_{D1}, with the isolated gate drive circuits, are switched. The switching of S_{C1} and S_{D1} provides the drive power for S_{C2} and S_{D2}. Then the drive power is sequentially supplied to the switches on the highest stage: S_{Cn} and S_{Dn}.

C. Comparison of the Number of Gate Drive Supplies

In this section, the number of isolated gate drive supplies is compared between the conventional DC/DC converters and the proposed isolation topology. For comparison, it is assumed that the volume of the proposed topology, which consists of the transformer and the rectifier, for each MOSFET is equivalent to the volume of the isolated DC/DC converter, which ensures the isolation of the input voltage of the Marx circuit. In addition, it is assumed that the isolation for the MOSFETs on the j-th stage is ensured by the series connections of the isolated DC/DC converters in the conventional system. Note that manufacturers do not guarantee the series connections of the isolated DC/DC converter. In the ideal condition, the common-mode voltage is equally divided among the series-connected DC/DC converters. On the contrary, the common-mode voltage is not equally divided because the parasitic capacitance between a primary and a secondary winding has a variation in practice.

First, the required number of isolated power supplies for the conventional system N_c is (1) for the n-stage Marx circuit, where $n \geq 2$.

$$N_c = \sum_{j=2}^{n} (2j-1) \tag{1}$$

On the other hand, the required number of isolated power supplies of the proposed topology is $N_p = 2(n - 1)$. For this reason, the volume of the proposed drive power supplies will be smaller than the conventional DC/DC converters connected in series. Note that the isolated power supply is required in the gate drive circuit for S_{C1} and S_{D1} regardless of the proposed or conventional method, as described above. Thus the power supplies for these switches are not counted into N_c and N_p.

III. Design of the Transformer Used for Power Supply

A. Modeling of Charging Current

In this section, the charging current for the gate drive circuit is modeled to design the transformer in order to supply the required power for gate drive circuits. The required gate drive power for each MOSFET is

$$P_{drive} = f_{sw} Q_g V_{gs} \tag{2},$$

where f_{sw} is the switching frequency of the Marx circuit, Q_g is the total gate charge of each MOSFET, and V_{gs} is the gate-source voltage during turn-on. The transformer supplies a sum of twice the power of (2) and power loss on the gate drive and optical receiver.

Fig. 2 shows the equivalent circuit at the start of the charging operation of the Marx circuit. In this consideration, it is

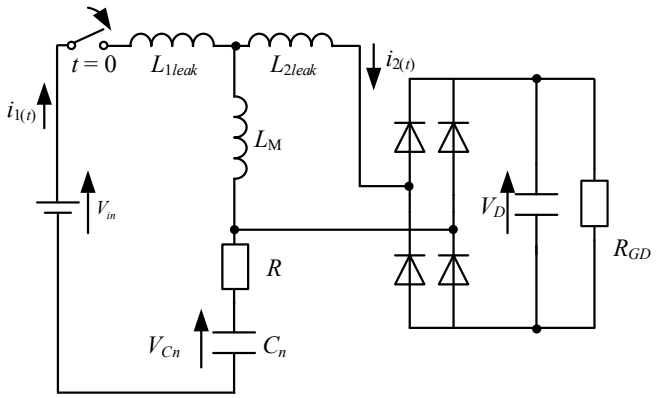

Fig. 2. Marx circuit with proposed gate drive circuits.

assumed that the primary inductance equals the secondary inductance for simplicity. The equivalent circuit consists of the input voltage V_{in}, the T-type equivalent circuit of the transformer Tr_n, the Marx capacitor C_n of each stage, the on-resistance R of the MOSFETs, and the load resistance emulating the gate drive circuit R_{GD}. The switch turns on at t = 0 at the start of charging mode. Here, the output power is expressed as

$$P_{GD} = f_{sw} V_D \int i_{2(t)} dt \tag{3}$$

where P_{GD} is the supplied power to the gate drive circuits, f_{sw} is the switching frequency of the Marx circuit, V_{Cn} is the Marx capacitor voltage, V_D is the DC voltage of the gate drive circuit, $i_{2(t)}$ is the current flowing on the secondary winding of the transformer in each stage.

The circuit equation is developed

$$\begin{cases} V_{in} - V_{Cn(0)} = L_{leak1}\dfrac{di_1}{dt} + L_M \dfrac{d(i_1 - i_2)}{dt} + \dfrac{1}{C_n}\int i_1 dt + Ri_1 \\ V_D = L_M \dfrac{d(i_2 - i_1)}{dt} + L_{leak2}\dfrac{di_2}{dt} \\ L_M = k\sqrt{L_1 L_2} \end{cases} \tag{4}$$

during the transient state, assuming the voltage drop of the Marx capacitor due to the previous discharging operation, where R is the equivalent resistance emulating the power consumption on the gate drive circuits, L_1 is the primary inductance, L_2 is the secondary inductance, L_M is the mutual inductance of the transformer, and $V_{Cn(0)}$ is the Marx capacitor voltage after the voltage drop by the discharging operation.

From (4), the secondary current $i_{2(t)}$ during the transient state is

$$i_{2(t)} = \frac{k\left(V_{in} - kV_D - V_{Cn(0)}\right)}{\sqrt{\dfrac{\beta}{C_n} - \left(\dfrac{R}{2}\right)^2}} e^{-\frac{R}{2\beta}t} \sin\sqrt{\frac{1}{\beta C_n} - \left(\frac{R}{2\beta}\right)^2}\, t - \frac{kV_D}{L_{1leak} + L_M} t \tag{5}$$

where β is

$$\beta = (L_{1leak} + L_M - kL_M) \tag{6}$$

V_D is the output voltage for gate drive circuits, and L_{1leak} is the leakage inductance of the primary inductance L_1.

The initial voltage of the Marx capacitor before the charging operation $V_{Cn(0)}$ is needed for the calculation of the $i_{2(t)}$. The voltage drop of each Marx capacitor is determined by the number of the stage. The theoretical output voltage without a load is

$$V_{out\_theory} = nV_{in} - V_{FD}\sum_{j=1}^{n-1} j \tag{7}$$

where V_{FD} is the forward voltage of the diodes, j is the number of times it passes through the diode. The forward voltage of the diodes should be considered because the voltage drop affects the charging current. During the charging period, the Marx capacitors are charged through multiple diodes. As a result, the Marx capacitor voltage of the upper stage is dropped due to the forward voltage drop of the diodes. When the capacitive load C_{out}, such as an ozonizer, is connected to the output of the Marx circuit, the output voltage is dropped due to the conservation law of the amount of charge. From the conservation law, (8) is developed.

$$\frac{1}{n}C_n V_{out\_theory} + C_{out}\left\{V_{in} - (n-1)V_{FD}\right\} = \left(\frac{1}{n}C_n + C_{out}\right)V_{out} \tag{8}$$

where V_{out} is the output voltage of the capacitive load C_{out}. From (8), the output voltage of the Marx circuit is

$$V_{out} = \frac{C_n V_{out\_theory} + nC_{out}\left\{V_{in} - (n-1)V_{FD}\right\}}{(C_n + nC_{out})} \tag{9}$$

As a result, the voltage drop of the capacitors after the discharging operation in each stage is

$$V_{cn(0)} = V_{in} - \frac{V_{out\_theory} - V_{out}}{n} \tag{10}$$

B. Design of Inductance for Transformer

The minimum inductance of the transformer is calculated from the current (5). The current $i_{2(t)}$ is approximated to solve the required inductance L analytically. As the approximation, the voltage drop by the on-resistance of the MOSFETs is ignored. Moreover, the proportional term to t in (5) is also ignored because the charging period of the Marx capacitor is in several microseconds. The effect of the proportional term is relatively small compared to the resonant term. The approximated current is

$$i_{2(t)} \approx \frac{k\left(V_{in} - kV_D - V_{Cn(0)}\right)}{\sqrt{\dfrac{\beta}{C_n} - \left(\dfrac{R}{2}\right)^2}} e^{-\frac{R}{2\beta}t} \sin\sqrt{\frac{1}{\beta C_n}}\, t \tag{11}$$

Figure 3 shows the calculated current i_2 expressed as (5) and its approximated current expressed as (11). In Fig. 3, the time when the approximated current takes the maximum and the maximum value are

$$t_2 \approx \frac{\sqrt{(L_{1leak} + L_M - kL_M)C_n}\,\pi}{2} \tag{12}$$

$$i_{\max} \approx \frac{k\left(V_{in} - kV_D - V_{Cn(0)}\right)}{\sqrt{\dfrac{L_{1leak} + L_M - kL_M}{C_n} - \left(\dfrac{R}{2}\right)^2}} \tag{13}$$

The time when the current takes the zero is

$$t_1 \approx \sqrt{(L_{1leak} + L_M - kL_M)C_n}\,\pi \tag{14}$$

The supplied power P_{GD} for two gate drive circuits is approximately calculated from the integral highlighted by the diagonal line in Fig. 3 with the base of t_1 and height of i_{max}.

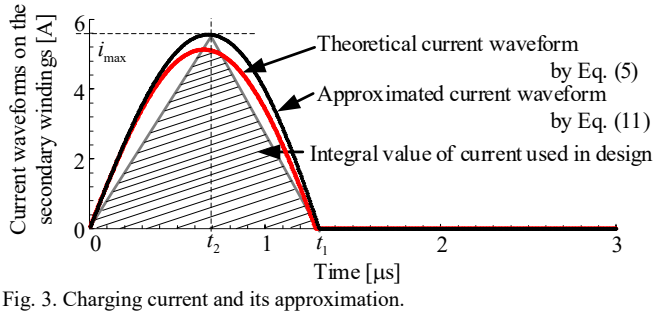

Fig. 3. Charging current and its approximation.

The supplied power to the secondary side is approximated as (15).

$$P_{GD} = f_{sw} V_{out} \frac{k\left(V_{in} - kV_D - V_{Cn(0)}\right)}{\sqrt{\frac{L_{1leak} + L_M - kL_M}{C_n} - \left(\frac{R}{2}\right)^2}} \sqrt{(L_{1leak} + L_M - kL_M)C_n}\,\pi \tag{15}$$

Since the self-inductance is the sum of leakage inductance L_{1leak} and mutual inductance L_M, the required self-inductance for the transformer is transformed from (15).

$$L_1 = \frac{C_n R^2 P_{GD}^2}{4\left(1-k^2\right)\left[P_{GD}^2 - \left\{f_{sw} C_n V_{out} \pi k \left(V_{in} - kV_D - V_{Cn(0)}\right)\right\}^2\right]} \tag{16}$$

IV. Experiments of Marx Circuit

In this chapter, the Marx circuit with the proposed gate drive circuits is demonstrated. Table I shows the specifications of the prototype.

A. Steady-State Operation

Fig. 4 shows the output voltage of the seven-stage Marx circuit with the proposed gate drive circuits. As the output voltage of the Marx circuit, an output voltage of 4 kV is obtained. Figs. 4 (b) and (c) are the expanded waveforms focusing on the positive and negative-going edge. The output voltage rises and falls within 100 ns. These results show that the proposed gate drive circuits are operating with high-output dv/dt.

Fig. 5 shows the charging operation of the gate drive circuit. At the start of the charging operation, the current flows on the secondary winding of the transformer as expressed by (5). Note that the positive current of i_2 at the start of the charging period is an unexpected current. Theoretically, the positive current never flows on the transformer at this time. Thus, the cause of the positive current is not known. However, it is possible that the noise caused by the high dv/dt at the start of the charging operation is interlinked on the current probe and observed as a current.

Fig. 6 shows the relation between the power and primary inductance when the gate drive voltage V_D is 16 V. The theoretical line calculated by (15) is drawn by the solid line and the simulation result is plotted by an open triangle. The circuit simulator PLECS (Plexim) is used for the simulation. The calculation and experimental results show that higher

TABLE I
Specifications of Prototype

Parameters	Symbols	Value
Input voltage	V_{in}	600 V
GDU voltage	V_D	16 V
Marx capacitor	C_n	0.22 µF
Switching frequency	f_{out}	10 kHz
on-resistance of MOSFETs	R	0.5 Ω
Coupling coefficient	k	0.95
Primary leakage inductance	L_{leak1}	(1-k)L_1
Secondary leakage inductance	L_{leak2}	(1-k)L_1
Primary inductor	L_1	10.5 µH
Magnetic core for trans.		PC44 (TDK)
Number of stage	n	7
Discharging time		6 µs
LED		SFH4542 (OSRAM) 7.7 × 6.0 × 4.8 mm
Photodiode		SFH2505 (OSRAM) 7.7 × 6.0 × 4.8 mm
MOSFETs		C3M0065100J (CREE)
Load	C_{out}	500 pF

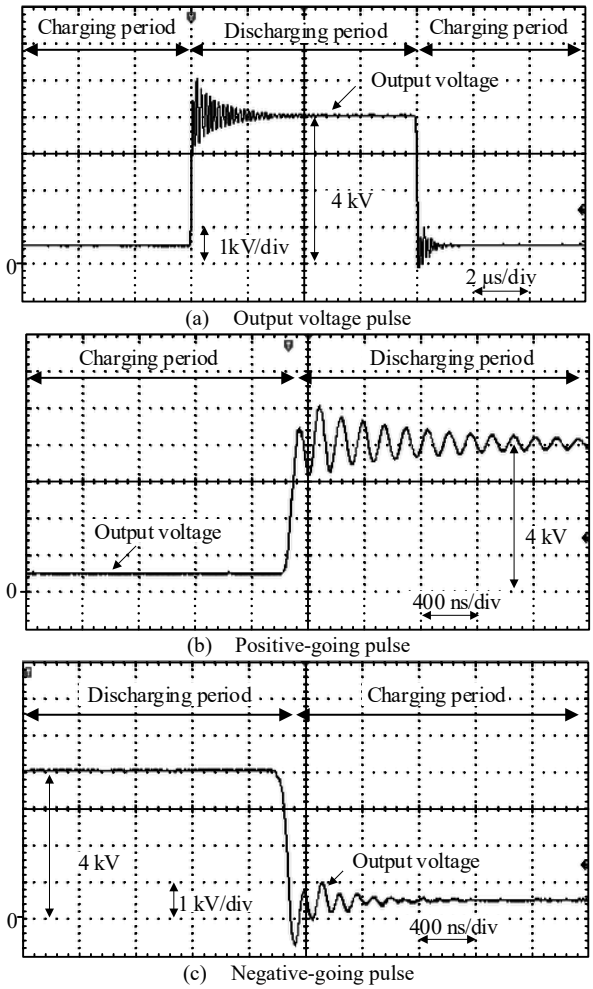

Fig. 4. Output voltage of the Marx circuit.

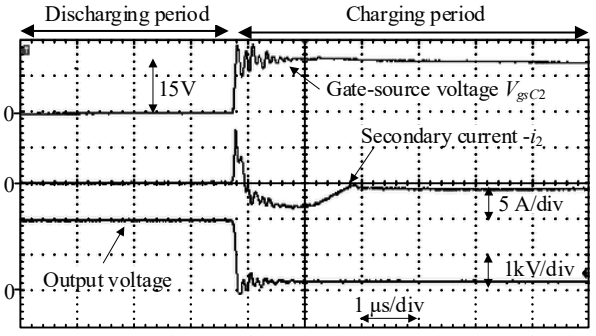

Fig. 5. Power supply for gate drive circuit via transformer at the charging period. The gate drive power is supplied using the charging current of the Marx capacitor.

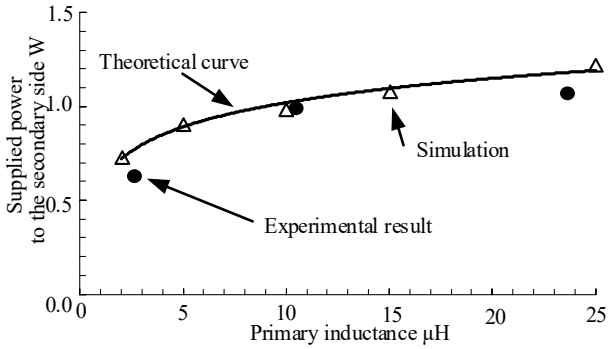

Fig. 6. Relation between supplied power to the gate drive circuit and primary inductance of the transformer.

inductance allows for supplying more power. This is because the current conduction time on the secondary side increases. The simulation results show good agreement with the theoretical curve. It means that the effects of the approximation related to (15) can be ignored. The obtained power in the experiments is slightly smaller than the simulation and the theoretical curve. In the above experiments, an inductance of 10.5 μH is used because the required gate drive power is less than 1.0 W for two MOSFETs.

B. Start-up Operation

Fig. 7 shows the start-up operation of the Marx circuit and the gate drive circuit. The start-up operation is tested with the reduced input voltage and reduced number of cells because of the limitation of the output current of the DC power supply. At 40 ms, an input voltage of 100 V is rapidly applied to the input of the Marx circuit. The MOSFETs S_{D1} and S_{C1} simultaneously start to switch because the gate drive circuits for S_{D1} and S_{C1} have the isolated DC-DC converter. Due to the charging current of the Marx capacitor C_1 by the switching of S_{D1} and S_{C1}, The gate drive power is supplied through the transformer Tr_1. After about 160 ms from the start-up, the gate drive voltage for S_{D2} reaches the nominal voltage: 15 V. Then, the drive power is sequentially supplied to the upper cell. These results show the proposed gate drive circuit does not need the isolated DC-DC converter except at the lowest stage.

C. Optical Isolation of Gate-drive Signal

Fig. 8 shows the gate signal transmission using LEDs and photodiodes. The LEDs and photodiodes are separately placed with an air gap of 50 mm. The air gap ensures the isolation distance between the controller on the low-voltage side and the gate drive circuits. The charging and the discharging signal are transmitted by the LEDs and photodiodes, as shown in (a). Fig. 8 (b) is the expanded waveforms of (a). The gate-source voltage for charging and discharging is about 500 ns delayed from the original signal from the controller.

V. CONCLUSION

In this paper, the self-powered gate drive circuits to reduce the cost for the Marx circuit of ozonizers have been proposed. The Marx circuit does not need an isolated auxiliary power supply for the gate drive circuits. The proposed self-powered gate drive circuits receive the drive power from the charging path of the

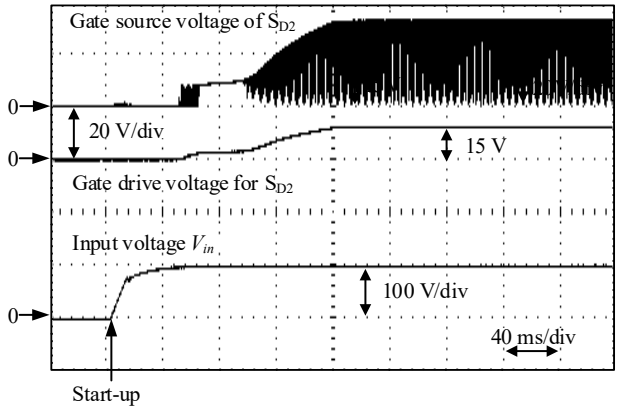

Fig. 7. Start-up operation of the Marx circuit and the gate drive circuits.

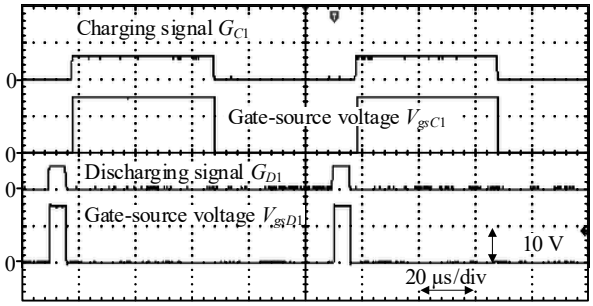

(a) Signal transmission for charging and discharging with optical isolation.

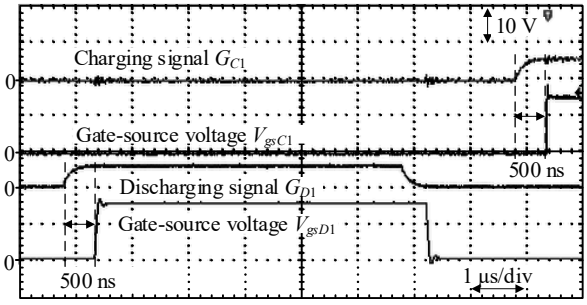

(b) Expanded waveforms of (a)

Fig. 8. Optical gate-signal transmission via LED and photodiode with isolation.

Marx circuit. The proposed gate drive circuit only requires a low withstand voltage because the power for the MOSFET on the n-th stage is supplied from the (n - 1)-th stage via a low-voltage transformer. Besides, the gate signal is transmitted through pairs of LEDs and photodiodes instead of optical fibers. The proposed gate drive circuits are developed and implemented into a prototype of the Marx circuit with an output voltage of 4 kV. From the experiments, it is demonstrated that the proposed drive circuits provide both drive power and gate signal.

REFERENCES

[1] P. Forzatti, L. Lietti, I. Nova, E. Tronconi, "Diesel NOx aftertreatment catalytic technologies: Analogies in LNT and SCR catalytic chemistry," Catalysis Today, Vol. 151, No. 3–4, pp. 202-211, Mar. 2010.

[2] M. Okubo, T. Kuroki, S. Kawasaki, K. Yoshida and T. Yamamoto, "Continuous Regeneration of Ceramic Particulate Filter in Stationary Diesel Engine by Nonthermal-Plasma-Induced Ozone Injection," IEEE Transactions on Industry Applications, Vol. 45, No. 5, pp. 1568-1574, Sept, 2009.

[3] M. Okubo, N. Arita, T. Kuroki, "Total Diesel Emission Control Technology Using Ozone Injection and Plasma Desorption," Plasma Chemistry and Plasma Processing, Vol. 28, pp. 173-187, Apr. 2008.
[4] H. Canacsinh, L. M. Redondo and J. F. Silva, "Marx-Type Solid-State Bipolar Modulator Topologies: Performance Comparison," in IEEE Transactions on Plasma Science, Vol. 40, No. 10, pp. 2603-2610, Oct. 2012.
[5] Ju Won Baek, Dong Wook Yoo, G. H. Rim and Jih-Sheng Lai, "Solid state Marx Generator using series-connected IGBTs," in IEEE Transactions on Plasma Science, Vol. 33, No. 4, pp. 1198-1204, Aug. 2005.
[6] T. Sakamoto and H. Akiyama, "Solid-State Dual Marx Generator With a Short Pulsewidth," IEEE Transactions on Plasma Science, Vol. 41, No. 10, pp. 2649-2653, Oct. 2013.
[7] T. Sakamoto, A. Nami, M. Akiyama and H. Akiyama, "A Repetitive Solid State Marx-Type Pulsed Power Generator Using Multistage Switch-Capacitor Cells," IEEE Transactions on Plasma Science, Vol. 40, No. 10, pp. 2316-2321, Oct. 2012.
[8] M. Bhatnagar and B. J. Baliga, "Comparison of 6H-SiC, 3C-SiC, and Si for power devices," IEEE Transactions on Electron Devices, vol. 40, no. 3, pp. 645-655, March 1993.
[9] J. Biela, M. Schweizer, S. Waffler and J. W. Kolar, "SiC versus Si—Evaluation of Potentials for Performance Improvement of Inverter and DC–DC Converter Systems by SiC Power Semiconductors," IEEE Transactions on Industrial Electronics, vol. 58, no. 7, pp. 2872-2882, July 2011
[10] D. Peftitsis, J. Rabkowski and H. Nee, "Self-Powered Gate Driver for Normally ON Silicon Carbide Junction Field-Effect Transistors Without External Power Supply," in IEEE Transactions on Power Electronics, vol. 28, no. 3, pp. 1488-1501 (2013)
[11] J. Garcia, E. Gurpinar and A. Castellazzi, "High-frequency modulated secondary-side self-powered isolated gate driver for full range PWM operation of SiC power MOSFETs," 2017 IEEE Applied Power Electronics Conference and Exposition (APEC), 2017, pp. 919-924, doi: 10.1109/APEC.2017.7930806.
[12] J. T. Strydom, M. A. de Rooij and J. D. van Wyk, "A comparison of fundamental gate-driver topologies for high frequency applications," Nineteenth Annual IEEE Applied Power Electronics Conference and Exposition, Vol. 2, pp. 1045-1052, Mar. 2004.
[13] Z. Ye, Y. Lei, W. Liu, P. S. Shenoy and R. C. N. Pilawa-Podgurski, "Improved Bootstrap Methods for Powering Floating Gate Drivers of Flying Capacitor Multilevel Converters and Hybrid Switched-Capacitor Converters," IEEE Transactions on Power Electronics, Vol. 35, No. 6, pp. 5965-5977, June 2020.

Keisuke Kusaka (S'13–M'16) was born in Miyagi, Japan in 1989. He received his B.S. and M.S. degrees in electrical, electronics and information engineering from Nagaoka University of Technology, Niigata, Japan in 2011, 2013, respectively. From 2015 to 2016, he was with Swiss Federal Institute of Technology in Lausanne (EPFL), Switzerland as a trainee. In 2016, he received his Ph.D. degree in energy and environment science from Nagaoka University of Technology. From 2016 to 2018, he was a postdoctoral researcher with Nagaoka University of Technology, Niigata, Japan. From 2018 to 2021, he was an assistant professor with the same university. He is currently a tenure track lecturer at Nagaoka University of Technology. His current research interests include the areas of wireless power transfer systems and high-frequency converters. Dr. Keisuke is a member of the Institute of Electrical Engineers of Japan and Society of Automotive Engineers of Japan. Dr. Keisuke received the second prize paper award in IPEC-Niigata 2018.

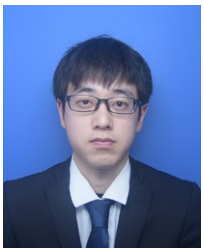

Yosuke Ouchi was born in Japan, in 1997. He received his B.S. degree from National Institute of Technology, Ibaraki College, Japan in 2019. In 2021, he received his M.S. degree in electrical, electronics and information engineering from Nagaoka University of Technology, Niigata, Japan.

Jun-ichi Itoh (M'04, SM'13) was born in Tokyo, Japan, in 1972. He received his M.S. and Ph.D. degree in electrical and electronic systems engineering from Nagaoka University of Technology, Niigata, Japan in 1996, 2000, respectively. From 1996 to 2004, he was with Fuji Electric Corporate Research and Development Ltd., Tokyo, Japan. He was with Nagaoka University of Technology, Niigata, Japan as an associate professor. Since 2017, he has been a professor. His research interests are matrix converters, dc/dc converters, power factor correction techniques, energy storage system and adjustable speed drive systems. He received IEEJ Academic Promotion Award (IEEJ Technical Development Award) in 2007. In addition, he also received Isao Takahashi Power Electronics Award in IPEC-Sapporo 2010 from IEEJ, 58th OHM Technology Award from The Foundation for Electrical Science and Engineering, November, 2011, Intelligent Cosmos Award from Intelligent Cosmos Foundation for the Promotion of Science, May, 2012, and Third prize award from Energy Conversion Congress and Exposition-Asia, June, 2013. Prizes for Science and Technology (Development Category) from the Commendation for Science and Technology by the Minister of Education, Culture, Sports, Science and Technology, April 2017. Dr. Itoh is a senior member of the Institute of Electrical Engineers of Japan, the Society of Automotive Engineers of Japan and the IEEE.